Toward an n-Type Molecular Wire: Electron Hopping within Linearly Linked Perylenediimide Oligomers

ARTICLE *in* JOURNAL OF THE AMERICAN CHEMICAL SOCIETY · AUGUST 2009

Impact Factor: 12.11 · DOI: 10.1021/ja902258g · Source: PubMed

J|A|C|S ARTICLES

Published on Web 06/09/2009

Toward an n-Type Molecular Wire: Electron Hopping within Linearly Linked Perylenediimide Oligomers

Thea M. Wilson,[†] Michael J. Tauber,[‡] and Michael R. Wasielewski*,[†]

Department of Chemistry and Argonne−Northwestern Solar Energy Research (ANSER) Center, Northwestern University, Evanston, Illinois 60208-3113, and Department of Chemistry and Biochemistry, University of California San Diego, La Jolla, California 92093-0314

Received March 22, 2009; E-mail: m-wasielewski@northwestern.edu

Abstract: A series of linearly linked perylenediimide (PDI) dimers and trimers were synthesized in which the PDI π systems are nearly orthogonal. These oligomers and several model compounds were singly reduced, and intramolecular electron hopping between the PDI molecules was probed by electron paramagnetic resonance (EPR) and electron nuclear double resonance (ENDOR) spectroscopy. When the functional groups attached to the ends of the oligomers were chosen to make each PDI molecule electronically equivalent, the single electron hops between the PDI molecules with rates that significantly exceed 10^7 s^{-1}. Rapid electron hopping between pairs of PDI molecules having orthogonal π systems is unexpected and may expand the possible design motifs for organic electronic materials based on PDI.

Introduction

Efficient charge transport among neighboring molecules is a requirement for the successful implementation of organic electronics, which have gained popularity because of their potential low-cost, ease of processability, and mechanical flexibility. Perylene-3,4:9,10-bis(dicarboximide) (PDI) and its derivatives have attracted significant interest as active materials for light harvesting,[1−4] photovoltaics,[5−12] and studies of basic photoinduced charge and energy transfer processes.[13−18] PDI is both photochemically and thermally stable[19] and can be easily modified at its imide nitrogens and its 1, 6, 7, and 12 positions. Modifications at these positions tune the electronic properties of PDI, resulting in derivatives that absorb light from the near-ultraviolet to the near-infrared region of the spectrum and that are either good electron acceptors[20] or donors.[21] PDI also demonstrates the ability to self-assemble in solution via hydrophobic/hydrophilic interactions as well as by $\pi-\pi$ stacking, a phenomenon which has been extensively studied in a variety of self-assembled, π-stacked PDI systems.[22−32] We have

[†] Northwestern University.
[‡] University of California, San Diego.

(1) Prathapan, S.; Yang, S. I.; Seth, J.; Miller, M. A.; Bocian, D. F.; Holten, D.; Lindsey, J. S. *J. Phys. Chem. B* **2001**, *105*, 8237–8248.
(2) Yang, S. I.; Prathapan, S.; Miller, M. A.; Seth, J.; Bocian, D. F.; Lindsey, J. S.; Holten, D. *J. Phys. Chem. B* **2001**, *105*, 8249–8258.
(3) Muthukumaran, K.; Loewe, R. S.; Kirmaier, C.; Hindin, E.; Schwartz, J. K.; Sazanovich, I. V.; Diers, J. R.; Bocian, D. F.; Holten, D.; Lindsey, J. S. *J. Phys. Chem. B* **2003**, *107*, 3431–3442.
(4) Baffreau, J.; Leroy-Lhez, S.; Van Anh, N.; Williams, R. M.; Hudhomme, P. *Chem.−Eur. J.* **2008**, *14*, 4974–4992.
(5) Chen, S.-G.; Stradins, P.; Gregg, B. A. *J. Phys. Chem. B* **2005**, *109*, 13451–13460.
(6) Chen, S. G.; Branz, H. M.; Eaton, S. S.; Taylor, P. C.; Cormier, R. A.; Gregg, B. A. *J. Phys. Chem. B* **2004**, *108*, 17329–17336.
(7) Gregg, B. A. *J. Phys. Chem. B* **2003**, *107*, 4688–4698.
(8) Neuteboom, E. E.; Meskers, S. C. J.; van Hal, P. A.; van Duren, J. K. J.; Meijer, E. W.; Janssen, R. A. J.; Dupin, H.; Pourtois, G.; Cornil, J.; Lazzaroni, R.; Bredas, J. L.; Beljonne, D. *J. Am. Chem. Soc.* **2003**, *125*, 8625–8638.
(9) Gregg, B. A.; Cormier, R. A. *J. Am. Chem. Soc.* **2001**, *123*, 7959–7960.
(10) Dittmer, J. J.; Marseglia, E. A.; Friend, R. H. *Adv. Mater.* **2000**, *12*, 1270–1274.
(11) Ferrere, S.; Zaban, A.; Gregg, B. A. *J. Phys. Chem. B* **1997**, *101*, 4490–4493.
(12) Tang, C. W. *Appl. Phys. Lett.* **1986**, *48*, 183–185.
(13) Ford, W. E.; Kamat, P. V. *J. Phys. Chem.* **1987**, *91*, 6373–6380.
(14) Ford, W. E.; Hiratsuka, H.; Kamat, P. V. *J. Phys. Chem.* **1989**, *93*, 6692–6696.
(15) Würthner, F.; Thalacker, C.; Sautter, A. *Adv. Mater.* **1999**, *11*, 754–758.
(16) Langhals, H.; Saulich, S. *Chem.−Eur. J.* **2002**, *8*, 5630–5643.
(17) Schenning, A.; Herrikhuyzen, J.; Jonkheijm, P.; Chen, Z.; Würthner, F.; Meijer, E. *J. Am. Chem. Soc.* **2002**, *124*, 10252–10253.
(18) Kirmaier, C.; Hindin, E.; Schwartz, J. K.; Sazanovich, I. V.; Diers, J. R.; Muthukumaran, K.; Taniguchi, M.; Bocian, D. F.; Lindsey, J. S.; Holten, D. *J. Phys. Chem. B* **2003**, *107*, 3443–3454.
(19) Pasaogullari, N.; Icil, H.; Demuth, M. *Dyes Pigm.* **2006**, *69*, 118–127.
(20) Ahrens, M. J.; Fuller, M. J.; Wasielewski, M. R. *Chem. Mater.* **2003**, *15*, 2684–2686.
(21) Zhao, Y.; Wasielewski, M. R. *Tetrahedron Lett.* **1999**, *40*, 7047–7050.
(22) Thalacker, C.; Würthner, F. *Adv. Funct. Mater.* **2002**, *12*, 209–218.
(23) Wurthner, F. *Chem. Commun.* **2004**, 1564–1579.
(24) Han, J. J.; Wang, W.; Li, A. D. Q. *J. Am. Chem. Soc.* **2006**, *128*, 672–673.
(25) Neuteboom, E. E.; Meskers, S. C. J.; Meijer, E. W.; Janssen, R. A. J. *Macromol. Chem. Phys.* **2004**, *205*, 217–222.
(26) Dehm, V.; Chen, Z.; Baumeister, U.; Prins, P.; Siebbeles, L. D. A.; Wuerthner, F. *Org. Lett.* **2007**, *9*, 1085–1088.
(27) Zhan, X.; Tan, Z.a.; Domercq, B.; An, Z.; Zhang, X.; Barlow, S.; Li, Y.; Zhu, D.; Kippelen, B.; Marder, S. R. *J. Am. Chem. Soc.* **2007**, *129*, 7246–7247.
(28) Che, Y.; Datar, A.; Balakrishnan, K.; Zang, L. *J. Am. Chem. Soc.* **2007**, *129*, 7234–7235.
(29) Che, Y.; Datar, A.; Yang, X.; Naddo, T.; Zhao, J.; Zang, L. *J. Am. Chem. Soc.* **2007**, *129*, 6354–6355.
(30) Yagai, S.; Monma, Y.; Kawauchi, N.; Karatsu, T.; Kitamura, A. *Org. Lett.* **2007**, *9*, 1137–1140.
(31) Chen, Z.; Baumeister, U.; Tschierske, C.; Wuerthner, F. *Chem.−Eur. J.* **2007**, *13*, 450–465.
(32) Zhang, J.; Hoeben, F. J. M.; Pouderoijen, M. J.; Schenning, A. P. H.; Meijer, E. W.; Schryver, F. C.; De Feyter, S. *Chem.−Eur. J.* **2006**, *12*, 9046–9055.

10.1021/ja902258g CCC: $40.75

recently investigated covalent PDI-based electron donor−acceptor systems that self-assemble to form larger structures for energy and electron transport.[33−36] Many of these systems take advantage of the tendency of these chromophores to form H-aggregates having roughly cofacial orientations. This promotes enhanced electronic communication between adjacent chromophores enabling efficient energy and/or charge transport.

The motivation for attaching molecules in linear arrays or rod-like assemblies has been extensively reviewed.[37] Prior elegant work has demonstrated efficient hole hopping within porphyrin arrays,[38] yet our knowledge of how molecular structure determines efficient charge hopping within a linear array of chromophores is not understood well enough to make predictions based on structure alone. To address the general question of electron transport within linear molecular arrays, we have examined a series of linear PDI dimers and trimers. Energy and charge migration along linear chains of rylene imides have been primarily explored by single molecule spectroscopy and by photoinduced intramolecular charge separation and recombination, which were found to occur with rates of $\sim 10^9$ s^{-1}.[39−46] This behavior is surprising given the nearly orthogonal orientation of the rylene π systems combined with the fact that both their HOMOs and LUMOs have nodes that bisect the N−N axis within each rylene, therefore minimizing the electronic coupling between the donor and acceptor rylenes. Questions remain, however, about the rate of charge migration between equivalent rylene sites, when an excess charge has been deposited into the oligomer by radiolysis, chemical, or electrochemical reduction. It is likely that the dependence of charge recombination rates within PDI-based electron donor−acceptor systems on the subtleties of molecular and electronic structure is different than the corresponding dependence of charge hopping rates between discrete monomer units within an oligomer.

In this study, we have used continuous wave electron paramagnetic resonance (EPR) and electron nuclear double resonance (ENDOR) techniques to explore electron hopping within monoreduced, directly linked PDI dimers and trimers. These two magnetic resonance techniques are very well-established as probes of charge hopping in both chemical and biological systems.[6,29,38,47−58] To enhance the solubility of PDI, as required for these solution phase studies, phenoxy groups were attached to the perylene core, as shown in Figure 1. Additionally, in an effort to make each of the PDI molecules electronically equivalent, the 2,6-diisopropylphenyl capping groups in the series **1a**−**3a** were replaced by naphthalimide groups in the series **1b**−**3b**. We find that electron hopping between PDI molecules is faster than the ENDOR time scale ($\sim 10^7$ s^{-1}) in both monoreduced dimers, **2a** and **2b**. We also observe electron hopping on the ENDOR time scale among all three PDI molecules in the linear trimer **3b**, a remarkable result given the node in the LUMO of PDI at the point at which it is attached to the neighboring PDI molecules. The results from these solution-phase studies point out possible new avenues of molecular design for organic charge transport materials that are

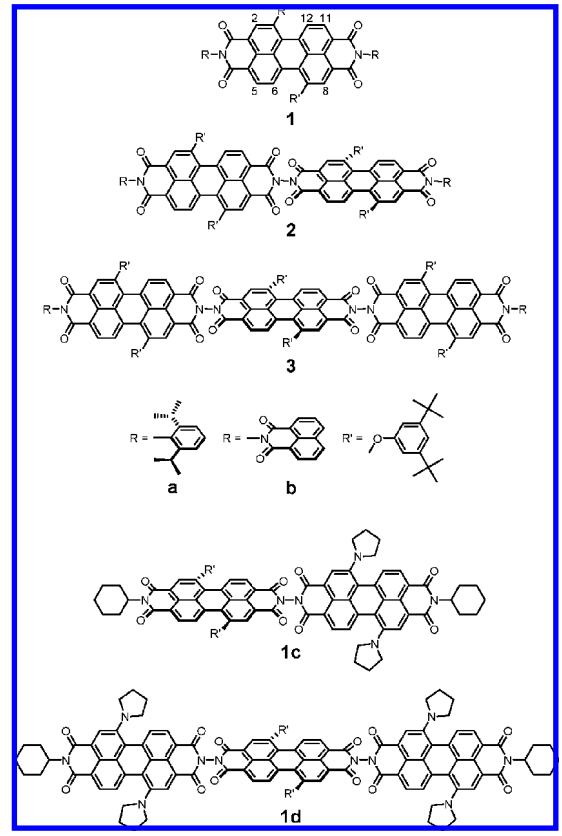

Figure 1. Structures of molecules.

(33) Ahrens, M. J.; Sinks, L. E.; Rybtchinski, B.; Liu, W. H.; Jones, B. A.; Giaimo, J. M.; Gusev, A. V.; Goshe, A. J.; Tiede, D. M.; Wasielewski, M. R. *J. Am. Chem. Soc.* **2004**, *126*, 8284–8294.
(34) Li, X. Y.; Sinks, L. E.; Rybtchinski, B.; Wasielewski, M. R. *J. Am. Chem. Soc.* **2004**, *126*, 10810–10811.
(35) Rybtchinski, B.; Sinks, L. E.; Wasielewski, M. R. *J. Am. Chem. Soc.* **2004**, *126*, 12268–12269.
(36) van der Boom, T.; Hayes, R. T.; Zhao, Y. Y.; Bushard, P. J.; Weiss, E. A.; Wasielewski, M. R. *J. Am. Chem. Soc.* **2002**, *124*, 9582–9590.
(37) Schwab, P. F. H.; Levin, M. D.; Michl, J. *Chem. Rev.* **1999**, *99*, 1863–1933.
(38) Susumu, K.; Frail, P. R.; Angiolillo, P. J.; Therien, M. J. *J. Am. Chem. Soc.* **2006**, *128*, 8380–8381.
(39) Giaimo, J. M.; Gusev, A. V.; Wasielewski, M. R. *J. Am. Chem. Soc.* **2002**, *124*, 8530–8531.
(40) Hernando, J.; Hoogenboom, J. P.; van Dijk, E. M. H. P.; Garcia-Lopez, J. J.; Crego-Calama, M.; Reinhoudt, D. N.; van Hulst, N. F.; Garcia-Parajo, M. F. *Phys. Rev. Lett.* **2004**, *93*, 236404.
(41) Holman, M. W.; Liu, R. C.; Zang, L.; Yan, P.; DiBenedetto, S. A.; Bowers, R. D.; Adams, D. M. *J. Am. Chem. Soc.* **2004**, *126*, 16126–16133.
(42) Holman, M. W.; Yan, P.; Adams, D. M.; Westenhoff, S.; Silva, C. *J. Phys. Chem. A* **2005**, *109*, 8548–8552.
(43) Hoogenboom, J. P.; Hernando, J.; van Dijk, E. M. H. R.; van Hulst, N. F.; Garcia-Parajo, M. F. *ChemPhysChem* **2007**, *8*, 823–833.
(44) Lukas, A. S.; Zhao, Y.; Miller, S. E.; Wasielewski, M. R. *J. Phys. Chem. B* **2002**, *106*, 1299–1306.
(45) Miller, S. E.; Schaller, R.; Mulloni, V.; Zhao, Y.; Just, E. M.; Johnson, R. C.; Wasielewski, M. R. *Chem. Phys.* **2002**, *275*, 167–183.
(46) Holman, M. W.; Adams, D. M. *ChemPhysChem* **2004**, *5*, 1831–1836.
(47) Gerson, F. *Top. Curr. Chem.* **1983**, *115*, 57–105.
(48) Muller, U.; Baumgarten, M. *J. Am. Chem. Soc.* **1995**, *117*, 5840–5850.
(49) Norris, J. R.; Uphaus, R. A.; Crespi, H. L.; Katz, J. *Proc. Natl. Acad. Sci. U.S.A.* **1971**, *68*, 625–628.
(50) Tauber, M. J.; Giaimo, J. M.; Kelley, R. F.; Rybtchinski, B.; Wasielewski, M. R. *J. Am. Chem. Soc.* **2006**, *128*, 1782–1783.
(51) Feher, G. *J. Chem. Soc., Perkin Trans. 2* **1992**, 1861–1874.
(52) McConnell, H. M. *J. Chem. Phys.* **1961**, *35*, 508–515.
(53) Norris, J. R.; Druyan, M. E.; Katz, J. J. *J. Am. Chem. Soc.* **1973**, *95*, 1680–1682.
(54) Weissman, S. I. *J. Am. Chem. Soc.* **1958**, *80*, 6462–6463.
(55) Huber, M.; Kurreck, H.; Von Maltzan, B.; Plato, M.; Möbius, K. *J. Chem. Soc., Faraday Trans.* **1990**, *86*, 1087–1094.
(56) Baumgarten, M.; Huber, W.; Mullen, K. *Adv. Phys. Org. Chem.* **1993**, *28*, 1–44.
(57) Holten, D.; Bocian, D. F.; Lindsey, J. S. *Acc. Chem. Res.* **2002**, *35*, 57–69.
(58) Thamyongkit, P.; Muresan, A. Z.; Diers, J. R.; Holten, D.; Bocian, D. F.; Lindsey, J. S. *J. Org. Chem.* **2007**, *72*, 5207–5217.

alternative or complementary to the predominant charge transfer routes mediated by intermolecular interactions based on $\pi-\pi$ stacking.

Experimental Section

Synthesis. The synthesis of **1c** has been described previously,[44] while the syntheses of the remaining molecules are detailed in the Supporting Information. Briefly, the PDI dimers and trimers were linked through N−N bonds at their imide groups via condensation of the monoanhydride of **1a**, first with hydrazine hydrate, followed by condensation of the resulting aminoimide with the appropriate mono- or dianhydride. The oligomers in series **1a**−**3a** are terminated with 2,6-diisopropylphenyl groups, while those in series **1b**−**3b** are terminated with naphthalene-1,8-dicarboximide (NMI). Molecules **1c**,**d** are terminated with cyclohexyl groups. Characterization was performed with a Varian INOVA 500 MHz NMR spectrometer and a PE Voyager DE-Pro MALDI-TOF mass spectrometer at Northwestern University (IMSERC). High-resolution mass spectra were obtained at Northwestern University and University of Illinois at Champaign−Urbana as described in the Supporting Information. Molecules **3a**, **3b**, and **1d** are mixtures of two diastereomers resulting from steric hindrance to rotation about the N−N bonds joining the PDI derivatives. These isomers proved difficult to separate, and their presence is only evident in broadening of the aromatic ^{1}H NMR resonances of the PDI derivatives. The presence of the isomers does not impact the studies described herein.

UV−Vis Spectroscopy and Electrochemistry. Steady-state absorption measurements were performed at room temperature on a Shimadzu 1601 UV/vis spectrometer. Spectra of the reduced species were obtained in the same 1.4 mm i.d. quartz tubes employed for EPR measurements. UV−vis and electrochemical measurements were performed in nonstabilized HPLC grade dichloromethane (DCM) (Fisher) or ACS reagent grade *N*,*N*-dimethylformamide (DMF) (Aldrich), which were dried using a Glass Contour solvent system. Electrochemical measurements were performed using a CH Instruments Model 622 electrochemical workstation. All measurements were performed in DCM containing 0.1 M tetrabutylammonium hexafluorophosphate ($TBAPF_6$) electrolyte. A 1.0 mm diameter platinum disk electrode, platinum wire counter electrode, and Ag/Ag_xO reference electrode were employed. The ferrocene/ferrocenium redox couple (Fc/Fc^+, 0.46 vs SCE)[59] was used as an internal reference for all measurements. $TBAPF_6$ was purchased from Aldrich and recrystallized twice from ethyl acetate prior to use.

EPR and ENDOR Spectroscopy. EPR and ENDOR spectra were acquired with a Bruker Elexsys E580 spectrometer, fitted with the DICE ENDOR accessory, EN801 resonator, and an ENI A-500 RF power amplifier. RF powers ranged from 200 to 400 W across the 7 MHz scanned range, and microwave power ranged from 2 to 20 mW. The sample temperature was controlled by a liquid nitrogen flow system. All samples and solvents were handled in a nitrogen atmosphere glovebox (MBraun Unilab). Samples were prepared in DMF with 1−4% triethylamine (TEA) (w/w) and loaded into 1.4 mm i.d. quartz tubes which were sealed with a 0.5−1.0 cm plug of vacuum grease and wrapped tightly with Parafilm. TEA was dried with CaH_2 and filtered through dry silica gel prior to use and storage in the glovebox. Photochemical reduction to form monoanions was accomplished by exciting the sample with an Ar^+ laser (514.5 nm, 40 mW) beam elongated in one dimension with a cylindrical lens. In all cases, the photochemical reductions using TEA formed solely monoanions of the PDI oligomers as monitored by UV−vis. UV−vis spectra acquired through the quartz tube match the spectra of PDI radical anions generated electrochemically. Reductions of the dimers and trimers were halted before 50 and 30% completion, respectively, to ensure maximum production of the singly reduced species. A spline fit baseline correction was applied to the ENDOR spectra following integration.

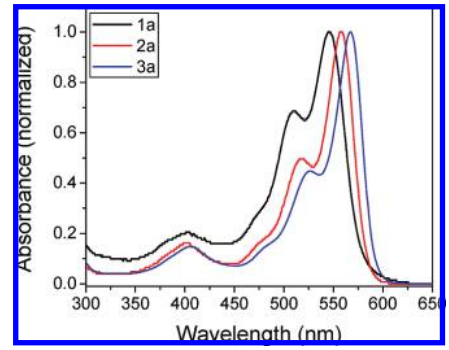

Figure 2. Normalized UV−vis absorption spectra of **1a**, **2a**, and **3a** in DCM.

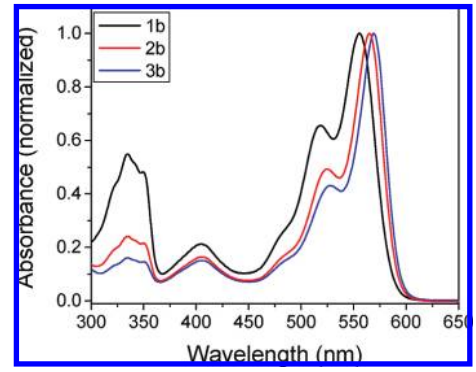

Figure 3. Normalized UV−vis absorption spectra of **1b**, **2b**, and **3b** in DCM.

Results

Steady-State Spectroscopy. The UV−vis absorption spectra of **1a**−**3a** and **1b**−**3b** are presented in Figures 2 and 3, respectively. The absorption maxima in each series red shift slightly with increasing oligomer length. These trends are similar to prior reports and are expected based upon exciton coupling of parallel, end-to-end transition dipoles of the PDI molecules.[44,45,60] Additionally, in both series, the absorption of the lowest energy peak in the vibronic progression is enhanced with an increase in the number of chromophores, also as expected from exciton coupling.[40,61,62] A representative radical anion absorption spectrum of **2a** is shown in Figure 4 (radical anion UV−vis spectra of **1a**, **3a**, and **1b**−**3b** are shown in Figures S1−S5 in Supporting Information). As the samples were photoreduced with TEA in DMF, anion bands at 725, ∼770 (shoulder), and 897 nm appeared and the vibronic progression in the visible region decreased in intensity, with the exciton-enhanced low-energy band diminishing more rapidly. Aggregation of the neutral species was not observed for any of the molecules in this study based upon comparisons of UV−vis spectra at concentrations ranging from dilute to saturated samples in solvents that included DCM, DMF, methylcyclohexane, and toluene.

Electrochemistry. Reduction potentials for both series are summarized in Table 1 and their differential pulse voltammo-

(59) Connelly, N. G.; Geiger, W. E. *Chem. Rev.* **1996**, *96*, 877–910.
(60) Langhals, H.; Ismael, R. *Eur. J. Org. Chem.* **1998**, *191*, 5–1917.
(61) Kasha, M.; Rawles, H. R.; El-Bayoumi, M. L. *Pure Appl. Chem.* **1965**, *11*, 371–392.
(62) Langhals, H.; Jona, W. *Angew. Chem., Int. Ed.* **1998**, *37*, 952–955.

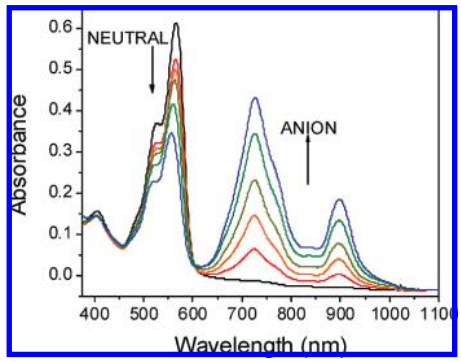

Figure 4. UV−vis absorption spectra of **2a** upon increasing (black, red, orange, ochre, green, blue) photochemical reduction with 514.5 nm light and TEA in DMF.

Table 1. Redox Potentials (V vs SCE)

peak	1a	2a	3a	1b	2b	3b
1[a]	−0.60	−0.55	−0.56	−0.56	−0.58	−0.58
2	−0.84	−0.75	−0.71	−0.73	−0.76	−0.77
3		−0.85	−0.82		−0.82	

[a] All PDI units are singly reduced, so $\mathbf{1}^{-}$, $\mathbf{2}^{2-}$, $\mathbf{3}^{3-}$.

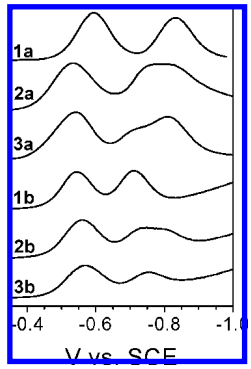

Figure 5. Differential pulse voltammograms.

grams presented in Figure 5. The first and second reduction potentials of **1a** are −0.60 and −0.84 V vs SCE, respectively. Dimer **1b** is slightly easier to reduce than **1a** by 0.04 V, and the relative difference between the first and second reduction potentials is also smaller in the **1b**−**3b** series. A third reduction can be distinguished near −0.8 V for both dimers; however, only two reduction steps are distinguished for **1a**, **1b**, and **3b**.

EPR and ENDOR Spectroscopy. The EPR spectra of all PDI radical anion species presented here are inhomogeneously broadened due to the large number of isotropic hyperfine coupling constants (hfcc's). While the hyperfine splittings in each of the monomer systems are partially resolved (Figure S6 in Supporting Information), those for the dimers are significantly broadened and both trimers exhibit a single unresolved line ($\mathbf{2b}^{\bullet-}$ and $\mathbf{3b}^{\bullet-}$ shown in Figure S9 in Supporting Information). Isotropic hfcc's (a_H) were obtained from ENDOR spectroscopy in liquid DMF at the ENDOR resonance condition $\nu^{\pm}_{ENDOR} = |\nu_n \pm a_H/2|$ where $\nu^{\pm}_{ENDOR}$ are the ENDOR transition frequencies and ν_n is the proton Larmor frequency.[63] The ENDOR spectra of $\mathbf{1a}^{\bullet-}$, $\mathbf{1c}^{\bullet-}$, and $\mathbf{2a}^{\bullet-}$ obtained at 290 K are presented in Figure 6. The monomer $\mathbf{1a}^{\bullet-}$ spectrum shows three well-defined line pairs with hfcc's of 5.0 (protons 6, 12), 2.1 (protons 5, 11),

(63) Kurreck, H.; Kirste, B.; Lubitz, W. *Electron Nuclear Double Resonance Spectroscopy of Radicals in Solution*; VCH: New York, 1988.

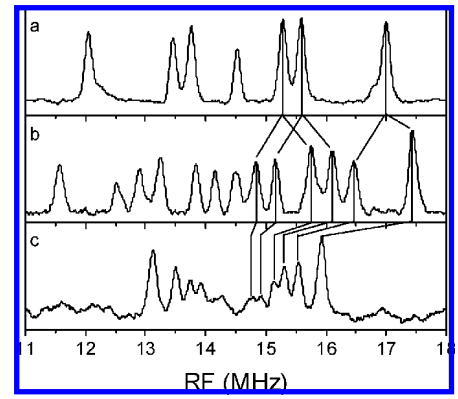

Figure 6. ^{1}H ENDOR spectra of $\mathbf{1a}^{\bullet-}$ (a), $\mathbf{1c}^{\bullet-}$ (b), and $\mathbf{2a}^{\bullet-}$ (c) in DMF with ∼1−4% TEA (w/w) at 290 K. Microwave powers were 2−20 mW, and RF power was 240−400 W with a frequency modulation depth of 100 kHz.

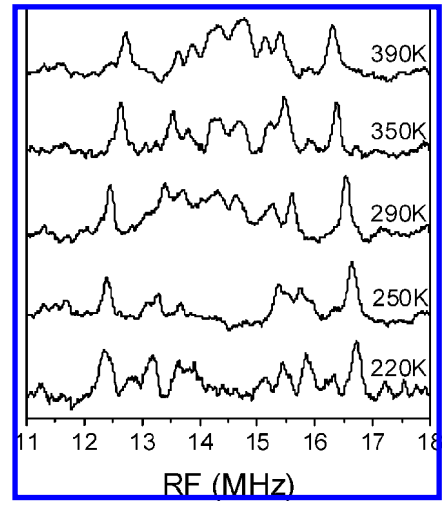

Figure 7. Temperature-dependent ^{1}H ENDOR spectra of $\mathbf{3a}^{\bullet-}$ in DMF with ∼1−4% TEA (w/w). Microwave power was 20 mW, and RF power 240−400 W with a frequency modulation depth of 100 kHz.

and 1.5 (protons 2, 8) MHz as previously assigned.[50] The additional single line at the proton Larmar frequency (14.5 MHz) is due to small unresolved hfcc's. The ENDOR spectrum of $\mathbf{1d}^{\bullet-}$ also has three paired lines with similar splittings of 4.8, 2.5, and 1.5 MHz (not shown). However, the spectrum of $\mathbf{1c}^{\bullet-}$ displays six line pairs, which result from a splitting of each proton resonance of $\mathbf{1a}^{\bullet-}$ by ∼1.9 MHz. The ENDOR spectrum of the linearly linked dimer $\mathbf{2a}^{\bullet-}$ also exhibits these extra splittings, but each hfcc is reduced by a factor of 2 (within 5%) compared to that of $\mathbf{1c}^{\bullet-}$, as shown in Figure 6c. There are no significant changes in the ENDOR spectrum of $\mathbf{2a}^{\bullet-}$ over the temperature range of 250−350 K (Figure S7 in Supporting Information). Unlike $\mathbf{2a}^{\bullet-}$, the ENDOR spectrum of $\mathbf{3a}^{\bullet-}$ changes significantly from 220 to 390 K, as shown in Figure 7. Among other changes, the overall spectral width narrows from 4.4 to 3.6 MHz as the temperature is increased from 220 to 390 K.

The proton ENDOR spectra of $\mathbf{1b}^{\bullet-}$, $\mathbf{2b}^{\bullet-}$, and $\mathbf{3b}^{\bullet-}$ at 290 K are presented in Figure 8. The spectrum of the NMI-capped monomer $\mathbf{1b}^{\bullet-}$ has hfcc's of 4.8, 2.6, and 1.8 MHz. The ENDOR spectrum of $\mathbf{2b}^{\bullet-}$ reveals hfcc's that are exactly half as large as those of $\mathbf{1b}^{\bullet-}$. While relative intensities and line widths of the peaks in the ENDOR spectra of the dimer depend significantly on temperature, the hfcc's are nearly unchanged over the liquid

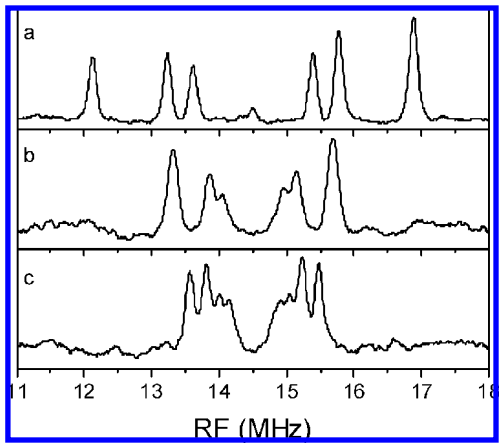

Figure 8. ^{1}H ENDOR spectra of **1b**$^{\bullet-}$ (a), **2b**$^{\bullet-}$ (b), and **3b**$^{\bullet-}$ (c) in DMF with ~1−4% TEA (w/w) at 290 K. Microwave powers were 2−6 mW, and RF power was 240−400 W with a frequency modulation depth of 100 kHz.

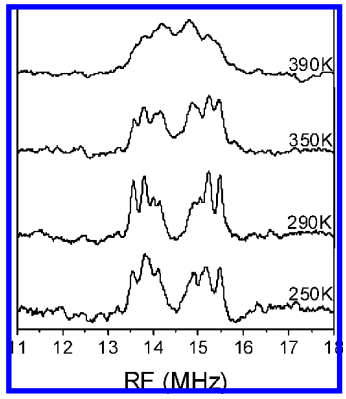

Figure 9. Temperature-dependent ^{1}H ENDOR spectra of **3b**$^{\bullet-}$ in DMF with ~1−4% TEA (w/w). Microwave powers were 2−20 mW, and RF power was 240−400 W with a frequency modulation depth of 100 kHz.

temperature range of DMF (Figure S8 in Supporting Information). The ENDOR spectrum of **3b**$^{\bullet-}$ has an overall spectral width of 1.9 MHz at 290 K. The temperature-dependent ENDOR spectra of **3b**$^{\bullet-}$ are shown in Figure 9, which also exhibit line broadening upon increasing temperature.

The EPR spectra of **1b**$^{\bullet-}$−**3b**$^{\bullet-}$ are presented in Figure S9 in Supporting Information. The second moments given in Table 2 were calculated from the measured first derivative signals using eq 1

$$\langle \Delta\omega^2 \rangle = \frac{\int_{-\infty}^{\infty} (\omega - \omega_{\text{center}})^2 f(\omega) \mathrm{d}\omega}{\int_{-\infty}^{\infty} f(\omega) \mathrm{d}\omega} \qquad (1)$$

where ω_{center} is the magnetic field at the center of the band and $f(\omega)$ is the experimentally measured spectrum. Experimental parameters were chosen to exclude broadening due to microwave saturation or over modulation. Calculations were repeated on 2−3 separate measurements to obtain averages.

Discussion

A qualitative and quantitative understanding of electron hopping in the linearly linked PDI oligomers benefits from comparisons made with model compounds **1a**−**d**. The results indicate that the ENDOR spectra of the radical anions strongly depend upon the number of linked PDI molecules, the symmetry of the PDI, and temperature. The radical anions used in these solution-phase EPR and ENDOR experiments are generated by photochemical reduction using a TEA sacrificial donor, which is closely monitored using UV−vis to ensure exclusive production of monoanions. The counterion is presumed to be TEAH$^+$ as described in the literature.[64,65] The use of a polar solvent, such as DMF, diminishes the potential effects of ion pairing, which might otherwise govern the nature of charge hopping/delocalization.[47,48,66] The spin density of **1a**$^{\bullet-}$ is substantial on the carbons nearest the bay region protons (6, 12 positions), as indicated by the large hfcc (5.0 MHz), which is assigned to those positions.[50] The central peak at 14.5 MHz, the ^{1}H Larmor frequency, found in the monomer spectra is attributed to small hfcc's from the *N*-(2,6-diisopropylphenyl), *N*-cyclohexyl, or 1,7-bis(3,5-di-*tert*-butylphenoxy) groups, or to solvent protons.

Table 2. Assignments of Hyperfine Coupling Constants (MHz) and Experimental Second Moments at 290 K

molecule	6,12 position	5,11 position	2,8 position	extra peaks[a]	$\langle \Delta\omega^2 \rangle$
1a	5.0	2.1	1.5	−	−
1b	4.8	2.6	1.8	−	2.74 ± 0.08
1c	5.9 4.0	3.2 1.3	2.5 0.7	−	−
1d	4.8	2.5	1.5	−	−
2a	2.8 2.0	1.6 0.8	1.2 0.5	−	−
2b	2.4	1.3	0.9	−	1.45 ± 0.05
3a	4.1	2.2	1.6	0.6 0.3	−
3a (390 K)	2.6	1.8	1.3	0.6 0.3	−
3b	1.9 1.4	1.0 0.8	~0.5	−	1.11 ± 0.06

[a] See text for assignment.

Reference compound **1c** is asymmetrically substituted at the two imide nitrogen atoms of PDI. The unpaired electron in **1c**$^{\bullet-}$ remains localized on the phenoxy-substituted PDI because the reduction potential of 1,7-bis(pyrrolidin-1-yl)-3,4:9,10-perylene-bis(dicarboximide) (5PDI) is 0.16 V more negative than PDI.[44] This asymmetric substitution perturbs the spin density distribution on the PDI as revealed in the ENDOR spectrum of **1c**$^{\bullet-}$ (Figure 6b), which has twice as many proton hfcc's compared to the symmetric monomers. In the case of reference molecule **1d**$^{\bullet-}$, PDI is again symmetrically substituted, so only three line pairs are observed in its ENDOR spectrum (not shown). However, it is noteworthy to mention that **1b**$^{\bullet-}$ and **1d**$^{\bullet-}$ have very similar ENDOR spectra, in which the two largest hfcc's of both compounds are ~4.8 and ~2.5 MHz. Our results suggest that the attachment of either NMI or 5PDI at the imide position of PDI alters the spin density distribution of PDI$^{\bullet-}$ in a similar manner.

The ENDOR spectrum of dimer **2a**$^{\bullet-}$ shown in Figure 6c displays six line pairs, as does the monomer reference compound **1c**$^{\bullet-}$. However, in the case of **2a**$^{\bullet-}$, the hfcc's are reduced by a factor of 2 compared to those of **1c**$^{\bullet-}$. This result shows unequivocally that the electron hops between the two PDI units in dimer **2a** at a rate that exceeds the ENDOR time scale (>10^7 s^{-1}). A recent study on monoreduced covalent and self-assembled π-stacked PDI molecules also reported halving of the spectral width when comparing the monomer to the dimers.[50] Therefore, on the EPR/ENDOR time scale, there is no distinction between the rates of electron transfer among cofacial and linear dimers of PDI. Although we anticipate the cofacial system to have the faster electron transfer

(64) Dapo, R.; Mann, C. K. *Anal. Chem.* **1963**, *35*, 677–680.
(65) Smith, P. J.; Mann, C. K. *J. Org. Chem.* **1969**, *34*, 1821–1826.
(66) Gerson, F.; Huber, W. *Electron Spin Resonance Spectroscopy of Organic Radicals*; Wiley-VCH: Weinheim, Germany, 2003.

rate due to greater orbital overlap, the actual rate has yet to be determined for either of these systems.

The ENDOR spectra of trimer **3a**$^{\bullet-}$ shown in Figure 7 display an overall reduction of the hfcc magnitudes; however, they are not reduced by a factor of 3 compared to a monomer reference molecule, as would be expected if the unpaired electron was hopping rapidly between all three units on the ENDOR time scale. Instead, the three outermost line pairs can be well-modeled by compressing the spectrum of **1a**$^{\bullet-}$ by up to 25% at the highest temperature measured (390 K), indicating that the radical anion is residing primarily on the central PDI of the linear trimer. The additional central peaks with splittings of 0.3 to 0.6 MHz are attributed to a small amount of spin leakage from the central PDI to the outer PDIs. The fact that the unpaired electron preferentially resides on the central PDI makes sense, given that the central PDI is attached to two electron-withdrawing imide groups which make it easier to reduce.

On the basis of the results in series **1a**−**3a**, the **1b**−**3b** series was designed with the goal of making each PDI as electronically similar as possible. Terminating the oligomers with NMI places electronically similar imide−imide bonds on both sides of each PDI. NMI acts as a second electron-withdrawing group on the termini of the PDI oligomers and is much more difficult to reduce (−1.3 V vs SCE) than PDI,[67] so that essentially no spin density resides on it. The capping of a PDI dimer or trimer with NMI groups should then make each PDI group effectively isoenergetic. The electrochemical data (Table 1) support the argument that NMI is more electron-withdrawing than 2,6-diisopropylphenyl because **1b** is easier to reduce than **1a** by 40 mV. Also, the observation that only one reduction wave is observed near the second reduction potential of **3b** while two separate waves are observed in **3a** indicates that the PDI molecules in **3b** have become nearly isoenergetic, as there is no longer a distinction between the outer and central PDI molecules in the **3b** trimer.

The ENDOR spectrum of **2b**$^{\bullet-}$ shown in Figure 8b, unlike that of **2a**$^{\bullet-}$, exhibits only three somewhat broadened line pairs. This demonstrates that the NMI capping group comes close to mimicking the electronic environment imposed by the direct linkage of PDI molecules via N−N bonds between their imide groups, such that the spin density distribution within each PDI in **2b**$^{\bullet-}$ is nearly symmetric. The hfcc's of **2b**$^{\bullet-}$ are exactly half of those of the monomer **1b**$^{\bullet-}$, leading to the conclusion that electron hopping on the ENDOR time scale occurs in this dimer as well as **2a**$^{\bullet-}$. The ENDOR spectrum of **3b**$^{\bullet-}$ (Figure 8c) shows that the presence of the NMI capping groups does not result in a completely symmetric spin distribution in the outer pair of PDI molecules. This is evidenced by the observed splitting of the ENDOR lines assigned to the 6,12, and 5,11 protons of the outer PDI in **3b**$^{\bullet-}$ (Figure 8c and Table 2). The unsplit lines due to the inner PDI as well as the small splittings due to the 2,8 protons are unresolved within the spectral envelope. The average of the resolved hfcc's for **3b**$^{\bullet-}$ shows that these splittings are one-third of the corresponding splittings of the monomer reference compound **1b**$^{\bullet-}$. As far as we are aware, this is the first example of an ENDOR spectrum narrowed by a factor of 3 for a linear trimer. Electron hopping in **3b**$^{\bullet-}$ at rates $>10^7$ s^{-1} is still observed upon lowering the temperature to 250 K.

Additionally, the number of sites over which a radical ion in a large π system hops or is delocalized on the EPR time scale can be determined by EPR line narrowing and second moment analysis.[49,68] According to the relationship set forth by Norris et al.,[49] $\langle\Delta\omega_N^2\rangle = 1/N\langle\Delta\omega_M^2\rangle$, the second moment of an EPR line in which the unpaired spin is delocalized over N molecules is proportional to $1/N$ times the second moment of the monomer. The experimentally determined second moments for **1b**$^{\bullet-}$−**3b**$^{\bullet-}$ listed in Table 2 follow an approximate $1/N$ relationship upon increasing the number of PDI molecules over which the unpaired electron is hopping.

UV−vis absorption spectra of the dimer and trimer radical anions as shown in Figure 4 and Figures S2 and S5 in Supporting Information show only minor perturbations due to electronic interactions between the chromophores, indicating that on the time scale of UV−vis absorption the unpaired electron is localized on a single PDI. Thus the electron hopping rate (k_{ET}) between the linearly linked PDI molecules lies in the regime between that of UV−vis absorption and ENDOR measurements (10^{14} s$^{-1} > k_{ET} > 10^7$ s^{-1}). This range is consistent with the rates determined for photoinduced charge transfer in similar systems.

Our model systems demonstrate that the relative energetics between neighboring PDI molecules (i.e., degeneracy) is crucial for efficient electron hopping in linearly linked PDIs. Electron hopping over longer oligomers is likely and could open the door to new types of architectures involving PDI molecules, namely, linear rather than π-stacked, for use in organic electronics. The fact that PDI molecules are also excellent absorbers of visible light, and that exciton coupling increases the extinction coefficient with increasing oligomer length, makes them also good candidates for solar cell applications.

Conclusions

Electron transfer among two different sets of monoreduced linearly linked, PDI oligomers having perpendicular π systems was studied using EPR and ENDOR spectroscopy. Electron hopping $>10^7$ s^{-1} was found to occur in both of the dimers. Despite the nodes in both the HOMO and LUMO of PDI that bisect its N−N axis, it was found that connecting PDI molecules via a N−N linkage at their imide groups results in a significant change in their reduction potential relative to attachment of alkyl substituents. In the case of the trimers, it was found that rapid electron hopping occurs only when all three PDI molecules are effectively isoenergetic, as afforded by the use of an NMI end-capping group. Our results indicate that linear PDI oligomers, and most likely those in the longer rylene diimide family, show promise as potential organic electronic materials for long distance electron transport.

Acknowledgment. This research was supported by the Chemical Sciences, Geosciences, and Biosciences Division, Office of Basic Energy Sciences, DOE under Grant No. DE-FG02-99ER14999. The authors would like to thank Dr. Yongyu Zhao for the synthesis of molecule **1c**, and Dr. Jovan Giaimo for the synthesis of molecule **1d**.

Supporting Information Available: Details regarding the synthesis and characterization of the molecules presented in this study and additional EPR/ENDOR data. This material is available free of charge via the Internet at http://pubs.acs.org.

JA902258G

(67) Viehbeck, A.; Goldberg, M. J.; Kovac, C. A. *J. Electrochem. Soc.* **1990**, *137*, 1460–1466.

(68) Vincow, G.; Johnson, P. M. *J. Chem. Phys.* **1963**, *39*, 1143–1153.